Mapping Local Nucleotide Flexibility by Selective Acylation of 2′-Amine Substituted RNA

Stacy I. Chamberlin and Kevin M. Weeks*

Contribution from the Department of Chemistry, University of North Carolina, Chapel Hill, North Carolina 27599-3290

Received April 29, 1999

Abstract: 2′-Amine substitutions in single-stranded oligoribonucleotides react more rapidly with activated esters than 2′-amine positions in mismatched or duplex RNA substrates. Reactivity does not reflect static solvent accessibility or electrostatics. We infer that acylation of 2′-amine substituted RNA is sensitive to local nucleotide flexibility. Selective acylation was used to map the structure and magnesium ion dependent conformational changes in $tRNA^{Asp}$ transcripts containing single 2′-amine substitutions per transcript. Under denaturing conditions, all 2′-amine substituted RNA positions show similar reactivity. When $tRNA^{Asp}$ transcripts are refolded under strongly native conditions (10 mM Mg^{2+}, 100 mM NaCl), positions involved in base pairing and known tertiary interactions, including base triples and loop−loop interactions, are protected from modification. In the absence of magnesium ion the acceptor, T- and anticodon stems form stable helices as judged by their low relative 2′-amine reactivity. In contrast, the D-stem and most tertiary interactions require greater than 1 mM $MgCl_2$ for stable folding. These results emphasize an interdependence between formation of the D-stem helix and tertiary structure folding for yeast $tRNA^{Asp}$ transcripts. This chemical approach for mapping local RNA flexibility yields results consistent with prior biophysical and biochemical studies emphasizing its utility for mapping local nucleotide environments on small quantities of RNA molecules of any size.

RNA folding is driven by several favorable processes including hydrogen bonding, base stacking, specific ion binding, and water and ion release.[1−3] Although there is a net global loss in nucleotide configurational entropy to achieve the folded state, individual RNA regions vary significantly in their local stability.[4] For example, base-paired helices and individual nucleotides involved in tertiary interactions are conformationally restrained, while hairpin loops may be locally dynamic.[5] Conformational changes upon ligand binding[6−8] and assembly with protein cofactors[9−11] further modulate local RNA stability. Methods that detect these changes in local stability are essential for understanding RNA folding and may lead to improvements in de novo RNA structure prediction.

Chemical and enzymatic footprinting techniques remain the principal methods for monitoring RNA conformational changes. Structural interactions can be inferred by monitoring reaction of individual bases with enzymatic,[12,13] electrophilic,[13−15] or oxidative reagents.[16,17] Modification is thought to monitor primarily static solvent accessibility, although reactivity may be modulated by electrostatic factors.[18] As many reagents and enzymes are selective for one or a few nucleotides, multiple, individually optimized experiments are required to monitor all positions within an RNA molecule. The solvent accessibility of the RNA backbone can be robustly monitored, at all residues, using hydroxyl radical cleavage.[19−21] Pb^{2+} cleaves the RNA backbone in a reaction governed by both backbone flexibility and sequence selective factors.[22,23]

Biophysical approaches yield valuable information regarding the extent of local residue flexibility. Temperature factors, obtained from crystallographic refinements, can be related to local residue flexibilities.[24,25] Detailed interpretation of crystallographic data is limited to high-resolution structures and can be complicated by crystal packing effects. Nuclear magnetic resonance techniques, such as imino proton exchange experiments, are sensitive to local motions including base flipping

* Corresponding author. E-mail: weeks@unc.edu.

(1) Serra, M. J.; Turner, D. H. *Methods Enzymol.* **1995**, *259*, 242−261.
(2) Cate, J. H.; Hanna, R. L.; Doudna, J. A. *Nat. Struct. Biol.* **1997**, *4*, 553−558.
(3) Conn, G. L.; Draper, D. E. *Curr. Opin. Struct. Biol.* **1998**, *8*, 278−285.
(4) Rigler, R.; Wintermeyer, W. *Annu. Rev. Biophys. Bioeng.* **1983**, *12*, 475−505.
(5) Jaeger, J. A.; Tinoco, I. *Biochemistry* **1993**, *3*, 12522−12530.
(6) Woodcock, J.; Moazed, D.; Cannon, M.; Davies, J.; Noller, H. F. *EMBO J.* **1991**, *10*, 3099−3103.
(7) Laing, L. G.; Gluick, T. C.; Draper, D. E. *J. Mol. Biol.* **1994**, *237*, 557−587.
(8) Feigon, J.; Dieckmann, T.; Smith, F. W. *Chem. Biol.* **1996**, *3*, 611−617.
(9) Allain, F. H.; Gubser, C. C.; Howe, P. W.; Nagai, K.; Neuhaus, D.; Varani, G. *Nature* **1996**, *380*, 646−650.
(10) Weeks, K. M. *Curr. Opin. Struct. Biol.* **1997**, *7*, 336−342.
(11) Patel, D. J. *Curr. Opin. Struct. Biol.* **1999**, *9*, 74−87.
(12) Ehresmann, C.; Baudin, F.; Mougel, M.; Romby, P.; Ebel, J.-P.; Ehresmann, B. *Nucleic Acids Res.* **1987**, *15*, 9109−9128.
(13) Knapp, G. *Methods Enzymol.* **1989**, *180*, 192−212.
(14) Peattie, D. A.; Herr, W. *Proc. Natl. Acad. Sci. U.S.A.* **1981**, *78*, 2273−2277.
(15) Moazed, D.; Stern, S.; Noller, H. F. *J. Mol. Biol.* **1986**, *187*, 399−416.
(16) Chen, X.; Woodson, S. A.; Burrows, C. J.; Rokita, S. E. *Biochemistry* **1993**, *32*, 7610−7616.
(17) Thorp, H. H. *Adv. Inorg. Chem.* **1995**, *43*, 127−177.
(18) Lavery, R.; Pullman, A. *Biophys. Chem.* **1984**, *19*, 171−181.
(19) Tullius, T. D.; Dombroski, B. A. *Proc. Natl. Acad. Sci. U.S.A.* **1986**, *83*, 5469−5473.
(20) Latham, J. A.; Cech, T. R. *Science* **1989**, *245*, 276−282.
(21) Sclavi, B.; Sullivan, M.; Chance, M. R.; Brenowitz, M.; Woodson, S. A. *Science* **1998**, *279*, 1940−1943.

10.1021/ja9914137 CCC: $19.00
Published on Web 12/30/1999

Scheme 1

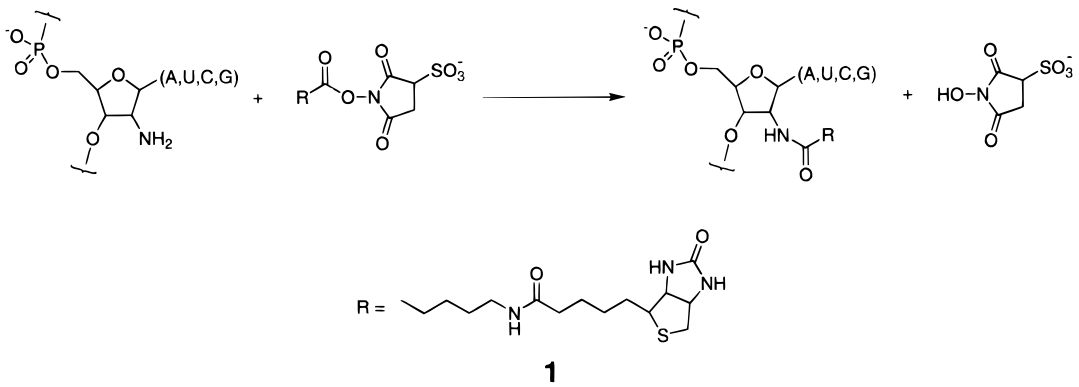

1

and helix−coil equilibria.[26,27] NMR studies are limited to small RNA systems or truncated versions of large RNAs. Tritium exchange experiments have been used to analyze structural changes upon ligand binding at purine residues.[28]

We have developed a general method for mapping local RNA stability that requires minimal optimization and can be used to monitor RNAs of any size at nucleotide resolution. RNA pools are generated containing, on average, a single 2′-amine substitution per transcript. Incorporation of a 2′-amine moiety introduces a reactive functionality within the RNA that can be selectively modified using an activated ester (Scheme 1).[29] Reaction yields the 2′-amide RNA product, which we detect as a stop to primer extension by reverse transcriptase. Remarkably, acylation of the 2′-amine position is gated by the underlying RNA structure. Thus, base-paired positions and nucleotides involved in tertiary interactions are less reactive than nucleotides located in less constrained loops. This approach provides a means for evaluating flexibility at single nucleotide resolution on small quantities of large RNAs.

Substitution of a 2′-amine group for the RNA 2′-hydroxyl is a chemically conservative change. Like the hydroxyl group, a primary amine functions as both a hydrogen bond donor and acceptor and has a comparable van der Waals radius.[30] The most significant difference lies in the preferred ribose pseudorotation angle. Isolated 2′-amine substituted nucleotides favor a C2′ endo sugar conformation (80% C2′), whereas ribonucleotides prefer the C3′ endo conformation (60% C3′).[31] Introduction of a single 2′-amine group destabilizes a nine base pair helix by 1.2 kcal/mol.[32] For the present study, these energetic effects are minimized since the energy barrier separating the two ribose conformations is low,[33] the energy of helix destabilization is small, and we employ tRNA transcripts that contain a single 2′-amine substituted nucleotide per RNA molecule. Single 2′-amine substitutions in the Tetrahymena[29] and hammerhead[34] ribozymes are structurally well tolerated.

Selective Acylation of 2′-Amine Positions in RNA. We evaluated the chemical selectivity of 2′-amine acylation using a model oligonucleotide substrate containing either all ribose nucleotides or a single 2′-amino-cytidyl substitution. The oligonucleotide substrate was treated with succinimidyl ester **1** (Scheme 1) and incorporation of the bulky biotinyl group was detected as a slowly migrating band in a denaturing polyacrylamide gel (Figure 1A). The all-ribose substrate reacts very slowly with the reagent (4% conversion in 60 min) as compared to the 2′-amine substituted oligonucleotide (97% conversion in 60 min). The slow baseline modification of the all-ribose substrate can be attributed to the reaction of base arylamines with the succinimidyl ester.[35,36]

Acylation is Governed by Local Nucleotide Flexibility. We compared acylation rates for single-stranded, duplex, and mismatched model substrates that each contained a single 2′-amino-cytidyl substitution in the center of a 20 residue oligonucleotide. The duplex contained 20 uninterrupted base pairs and the mismatched duplex contained a single C:A mismatch at the site of the 2′-amine substituted nucleotide (see Experimental Section). Acylation of the single-stranded oligoribonucleotide is efficient and characterized by a pseudo-first-order rate constant of 0.13 min^{-1} at 50 mM ester (circles in Figure 1B). In contrast, acylation is 5- and 12-fold slower for the mismatched ($k_{obs} \approx 0.027$) and fully base-paired ($k_{obs} \approx 0.011$) substrates, respectively (Figure 1B, squares and triangles, respectively; see also series 2 in Table 1). Thus, acylation is sensitive to local RNA structure at the site of the unique 2′-amine substituted nucleotide.

We tested the sensitivity of the acylation reaction to increasing magnesium ion concentrations. Acylation rates are essentially independent of magnesium ion concentration between 0 and 50 mM divalent ion (Table 1, series 1−3). Reactions of the duplex and single-stranded substrates were identical, within error, at all magnesium ion concentrations, while reactions of the mismatched substrate varied by less than 1.5-fold. These results indicate that acylation is insensitive to the electrostatic environment as governed by $MgCl_2$ concentration. Since higher-order RNA folding is often magnesium ion dependent, selective acylation of 2′-amine substituted nucleotides can be used to monitor RNA folding transitions.

(22) Ciesiolka, J.; Michalowski, D.; Wrzesinski, J.; Krajewski, J.; Krzyzosiak, W. J. *J. Mol. Biol.* **1998**, *275*, 211−220.
(23) Perret, V.; Garcia, A.; Puglisi, J.; Grosjean, H.; Ebel, J. P.; Florentz, C.; Giege, R. *Biochimie* **1990**, *72*, 735−744.
(24) Northrup, S. H.; Pear, M. R.; McCammon, J. A.; Karplus, M.; Takano, T. *Nature* **1980**, *287*, 659−660.
(25) Kuriyan, J.; Weis, W. I. *Proc. Natl. Acad. Sci. U.S.A.* **1991**, *88*, 2773−2777.
(26) Reid, B. R. *Annu. Rev. Biochem.* **1981**, *50*, 969−996.
(27) Figueroa, N.; Keith, G.; Leroy, J.; Plateau, P.; Roy, S.; Gueron, M. *Proc. Natl. Acad. Sci. U.S.A.* **1983**, *80*, 4330−4333.
(28) Gamble, R. C.; Schoemaker, H. J. P.; Jekowsky, E.; Schimmel, P. R. *Biochemistry* **1976**, *15*, 2791−2799.
(29) Cohen, S. B.; Cech, T. R. *J. Am. Chem. Soc.* **1997**, *119*, 6259−6268.
(30) Hobbs, J.; Sternback, H.; Sprinzl, M.; Eckstein, F. *Biochemistry* **1973**, *12*, 5138−5145.
(31) Guschlbauer, W.; Jankowski, K. *Nucleic Acids Res.* **1980**, *8*, 1421−33.
(32) Aurup, H.; Tuschl, T.; Benseler, F.; Ludwig, J.; Eckstein, F. *Nucleic Acids Res.* **1994**, *22*, 20−24.
(33) Saenger, W. *Principles of Nucleic Acid Structure*; Springer-Verlag: New York, 1984.
(34) Heidenreich, O.; Benseler, F.; Fahrenholz, A.; Eckstein, F. *J. Biol. Chem.* **1994**, *269*, 2131−2138.
(35) Staros, J. V.; Wright, R. W.; Swingle, D. M. *Anal. Biochem.* **1986**, *156*, 220−222.
(36) Millan, K. M.; Mikkelsen, S. R. *Anal. Chem.* **1993**, *65*, 2317−2323.

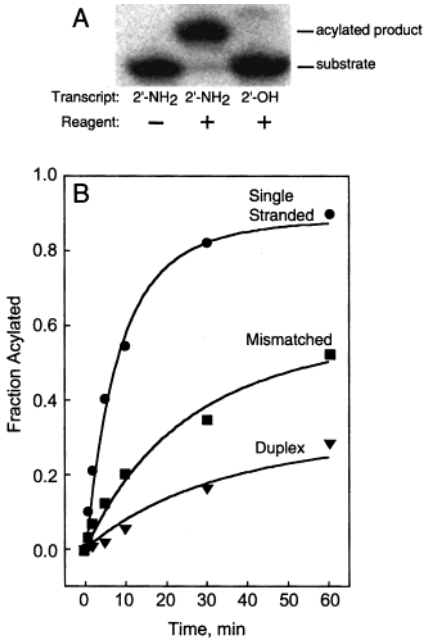

Figure 1. Selective acylation of 2′-amine substituted nucleotides as a function of RNA structure. (A) Acylation is selective for 2′-amine positions in RNA. A ^{32}P-labeled oligonucleotide containing either all 2′-hydroxyl nucleotides or a single 2′-amino-cytidyl substitution was treated with **1** (50 mM) in 10 mM $MgCl_2$, 100 mM NaCl at 37 °C for 60 min. The acylated product is resolved as a band with reduced mobility in the denaturing gel. (B) Rate of acylation is dependent upon local nucleotide flexibility. Acylation rates were determined for single-stranded, single nucleotide mismatched, and duplex substrates. The single stranded substrate (k_{obs} = 0.13 min^{-1}, circles) reacts approximately 5- and 12-fold faster than the mismatched (k_{obs} = 0.027 min^{-1}, squares) and duplex (k_{obs} = 0.011 min^{-1}, triangles) substrates, respectively. Curves represent a best fit to an equation that takes into account parallel reaction of the activated ester via hydrolysis and RNA acylation (see Experimental).

Table 1. Acylation Rates of Single 2′-Amino Substituted Oligonucleotide RNA Substrates[a]

series	[$MgCl_2$], mM	reagent,[b] mM	k_{obs}, min^{-1} duplex	mismatched	single-stranded
1	0	Anionic, 50 mM	0.0088	0.024	0.12
2	10	Anionic, 50 mM	0.011	0.027	0.13
3	50	Anionic, 50 mM	0.0092	0.033	0.12
4	0	Anionic, 20 mM[c]	0.0043	0.013	0.070
5	0	Neutral, 20 mM	0.0041	0.018	0.086

[a] Reactions were performed in 100 mM HEPES/sodium acetate/MES (pH8.0), 100 mM NaCl and the indicated [$MgCl_2$]. [b] Anionic refers to **1**, as shown in Scheme 1, and neutral refers to the ester analogue lacking the sulfonate moiety. [c] Lower reagent concentrations were used in reactions 4 and 5 due to the limited solubility of the neutral ester in aqueous solution.

We tested further electrostatic contributions to the selectivity of 2′-amine acylation by altering the reagent charge. The anionic (sulfo) succinimidyl ester was used in our experiments (Scheme 1), due to the reagent's increased solubility in aqueous solution. To test whether reactivity is effected by a repulsive interaction between the reagent and the RNA backbone, we monitored the rate of acylation using the neutral form of the activated ester, succinimidyl-6-(biotinamido)hexanoate. Single-stranded, duplex, and mismatched substrates are acylated at similar rates using either the anionic or neutral reagent (Table 1, compare series 4 and 5).

What governs the rate of acylation for 2′-amine substituted RNAs? Crystallographic data indicate that the 2′-ribose position at both base-paired and mismatched positions has similar static solvent accessibilities.[37−40] Acylation is insensitive to magnesium ion concentration or reagent charge (Table 1), demonstrating that electrostatic factors do not control acylation selectivity. The central difference between our model substrates is local nucleotide flexibility. Single-stranded and mismatched positions experience a greater range of motion than positions involved in base pairs or other stabilizing interactions.[41,42] We infer that 2′-amine acylation monitors local nucleotide flexibility and can be used to map nucleotide stabilities in larger RNA systems. We exploit this approach to study local nucleotide flexibility and magnesium ion-induced conformational changes in tRNA^{Asp} transcripts.

tRNA^{Asp}. Our studies focus on yeast tRNA^{Asp}, due to the wealth of supporting biochemical and structural information including chemical footprinting experiments,[23,43] NMR studies,[44,45] and crystallographic refinements.[46,47] The higher-order folding of tRNA^{Asp} is stabilized by magnesium ion binding and involves coaxial stacking of short RNA helices and a network of tertiary interactions to form a characteristic L-shaped molecule.[46,48]

The tRNA^{Asp} transcripts used in these experiments were generated by in vitro transcription using T7 RNA polymerase[49] and contained two sequence changes relative to wild type. The U1:A72 base pair was changed to a G−C base pair to facilitate efficient transcription, and a 20 nucleotide primer binding site was appended to the 3′-end of the RNA (Figure 2). Since these RNAs were generated by in vitro transcription, the eight modified nucleotides (ribothymidine, pseudouridine, dihydrouridine, 5-methylcytosine, and 1-methylguanine) found in the native RNA are substituted with U, C, and G, respectively.

The predicted lowest free-energy secondary structure[50] for this transcript is identical to that for wild-type yeast tRNA^{Asp}. tRNA^{Asp} transcripts lacking modified nucleotides and containing the G1:C72 base pair change are efficiently aminoacylated by tRNA^{Asp} synthetase.[51,52] While the modified bases are not essential for proper three-dimensional folding under strongly native conditions, their removal does destabilize the tertiary fold relative to the native RNA.[23,53]

(37) Pan, B.; Mitra, S. N.; Sun, L.; Hart, D.; Sundaralingam, M. *Nucleic Acids Res.* **1998**, *26*, 5699−5706.
(38) Pan, B.; Mitra, S. N.; Sundaralingam, M. *J. Mol. Biol.* **1998**, *283*, 977−984.
(39) Pan, B.; Mitra, S. N.; Sundaralingam, M. *Biochemistry* **1998**, *38*, 2826−2831.
(40) Jang, S. B.; Hung, L.-W.; Chi, Y.-I.; Holbrook, E. L.; Carter, R. J.; Holbrook, S. R. *Biochemistry* **1998**, *37*, 11726−11731.
(41) Varani, G.; Wimberly, B.; Tinoco, I. *Biochemistry* **1989**, *28*, 7760−7772.
(42) Fazakerley, V.; Boulard, Y. *Methods Enzymol.* **1995**, *261*, 145−163.
(43) Romby, P.; Moras, D.; Dumas, P.; Ebel, J. P.; Giege, R. *J. Mol. Biol.* **1987**, *195*, 193−204.
(44) Roy, S.; Papastavros, M. Z.; Redfield, A. G. *Biochemistry* **1982**, *21*, 6081−6088.
(45) Choi, B. S.; Redfield, A. G. *J. Biochem.* **1995**, *117*, 515−520.
(46) Westhof, E.; Dumas, P.; Moras, D. *J. Mol. Biol.* **1985**, *184*, 119−145.
(47) Westhof, E.; Dumas, P. H.; Moras, D. *Acta Crystallogr.* **1988**, *A 44*, 112−123.
(48) Kim, S. H.; Sussman, J. L.; Suddath, F. L.; Quigley, G. J.; McPherson, A.; Wang, A. H.; Seeman, N. C.; Rich, A. *Proc. Natl. Acad. Sci. U.S.A.* **1974**, *71*, 4970−4974.
(49) Milligan, J. F.; Uhlenbeck, O. C. *Methods Enzymol.* **1989**, *180*, 51−62.
(50) Jaeger, J. A.; Turner, D. H.; Zuker, M. *Proc. Natl. Acad. Sci. U.S.A.* **1989**, *86*, 7706−7710.
(51) Perret, V.; Garcia, A.; Grosjean, H.; Ebel, J. P.; Florentz, C.; Giege, R. *Nature* **1990**, *344*, 781−789.
(52) Sissler, M.; Eriani, G.; Martin, F.; Geige, R.; Florentz, C. *Nucleic Acids Res.* **1997**, *25*, 4899−4906.

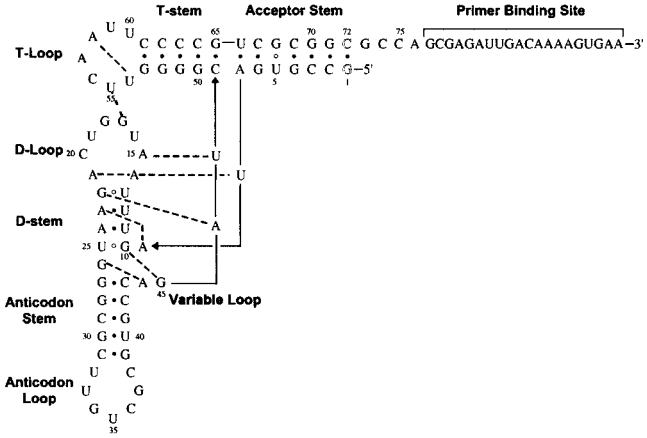

Figure 2. Schematic representation of the yeast tRNA^{Asp} transcript. Structure is drawn to suggest arrangement of base-paired helices and tertiary interactions in three dimensions.[48] Base pairs are shown as dots, tertiary interactions as dashed lines. U1:A72 was changed to a G−C pair (in outline) to facilitate efficient transcription.[49] Transcript also contains 20 noncoded nucleotides appended at the 3′ end to serve as a primer binding site.

Specificity and Detection of Acylation in tRNA^{Asp} Transcript Pools. RNAs containing 2′-amino pyrimidine nucleotides are used efficiently as templates by reverse transcriptase to direct cDNA synthesis.[54,55] We demonstrate that RNAs containing 2′-amino purine nucleotides also serve as templates for reverse transcriptase and show that the 2′-amide product obtained following selective acylation causes a stop to primer extension by reverse transcriptase.

tRNA^{Asp} transcripts were generated in which one nucleotide (A, U, C, or G) was substituted with its 2′-amine analogue to yield, on average, a single substitution per transcript. To test the selectivity of the acylation chemistry and to evaluate the level of 2′-amine substitution in tRNA^{Asp} transcripts, RNAs were modified quantitatively under denaturing conditions (50% (v/v) formamide). We compared primer extension reactions[56] performed with 2′-amine substituted RNA or 2′-amide (acylated) RNA templates to a conventional sequencing ladder generated by dideoxy chain termination (Figure 3). Reverse transcriptase efficiently extends the 2′-amine substituted templates, including those containing 2′-amino purines (Figure 3, panel A). In contrast, primer extension of 2′-acylated tRNA^{Asp} transcripts yields a clear sequencing ladder comparable in quality to that produced by dideoxy chain termination (Figure 3, compare panels B and C). Thus, cDNA synthesis by reverse transcriptase is impeded by the acylated product, but not by templates containing the 2′-amine substitution itself. In addition, acylation produces uniform band intensities over the entire cDNA ladder confirming that, first, acylation is specific for 2′-amino nucleotides and, second, the tRNA^{Asp} transcript pools contain approximately single 2′-amino-2′-deoxy nucleotide substitutions per transcript.

Acylation of 2′-Amine Substituted RNA is Sensitive to Secondary and Tertiary Structure. We compared the relative reactivities of 2′-amine substituted tRNA^{Asp} transcripts under solution conditions designed (i) to denature completely the RNA (50% (v/v) formamide, 1 mM EDTA) and (ii) to stabilize the native tertiary structure (10 mM $MgCl_2$, 100 mM NaCl) (Figure 4). Reaction under denaturing conditions established the reactivity of 2′-amine substituted positions in unstructured RNA and controlled for differences in band intensities attributable to primer extension.

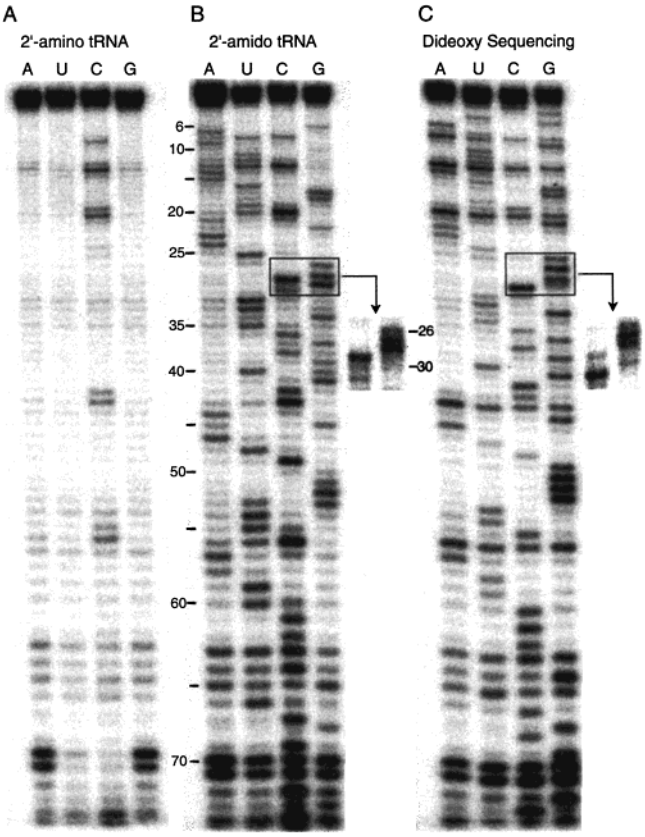

Figure 3. Detecting 2′-acylated tRNA products by primer extension. Pools of RNA were generated containing, on average, a single 2′-amine substitution per transcript. Primer extension reactions were performed on (A) the unmodified 2′-amine containing transcripts or on (B) 2′-amido (acylated) transcripts. Sequencing lanes (C) were generated by primer extension in the presence of chain-terminating dideoxy nucleotides. For panel B, tRNA^{Asp} was treated with **1** (see Scheme 1) under denaturing conditions. Bands in the G26 to C31 region (boxed) are not fully separated on a 7 M urea, denaturing polyacrylamide gel, but are resolved in a gel containing formamide (inset). Note that stops caused by the 2′-amido lesion are offset by one position relative to the bands generated by dideoxy sequencing.

Under conditions that stabilize native folding of tRNA^{Asp}, specific positions become protected from acylation as compared with reaction under denaturing conditions (identified with arrowheads in Figure 4). For example, in reactions of transcripts containing 2′-amino-guanosine, four consecutive G residues, within the T-stem (positions 50−53), show significant protection (Figure 4, G lanes). Residues involved in tertiary interactions, such as the interaction of G45 in the variable loop with the G10:U25 base pair, are also strongly protected. In addition, the method accurately identifies the A15:U48 Levitt pair, the intraloop A14 to A21 and U54 to A58 interactions, and the base triple interaction of A21 with the reverse Hoogsten pair U8:A14. In contrast, positions such as G34, C56, and U32 exhibit little or no change in reactivity between native and denaturing conditions. These reactive residues are located in flexible loop regions and do not participate in tertiary contacts as judged from the crystal structure.[46]

(53) Maglott, E. J.; Deo, S. S.; Przykorska, A.; Glick, G. D. *Biochemistry* **1998**, *37*, 16349−16359.
(54) Jellinek, D.; Green, L. S.; Bell, C.; Lynott, C. K.; Gill, N.; Vargeese, C.; Kirschenheuter, G.; McGee, D. P. C.; Abesinghe, P.; Pieken, W. A.; Shapiro, R.; Rifkin, D. B.; Moscatelli, D.; Janjic, N. *Biochemistry* **1995**, *34*, 11363−11372.
(55) Kujau, M. J.; Wolfl, S. *Nucleic Acids Res.* **1998**, *26*, 1851−1853.
(56) Niranjanakumari, S.; Stams, T.; Cray, S. M.; Christianson, D. W.; Fierke, C. A. *Proc. Natl. Acad. Sci. U.S.A.* **1998**, *95*, 15212−15217.

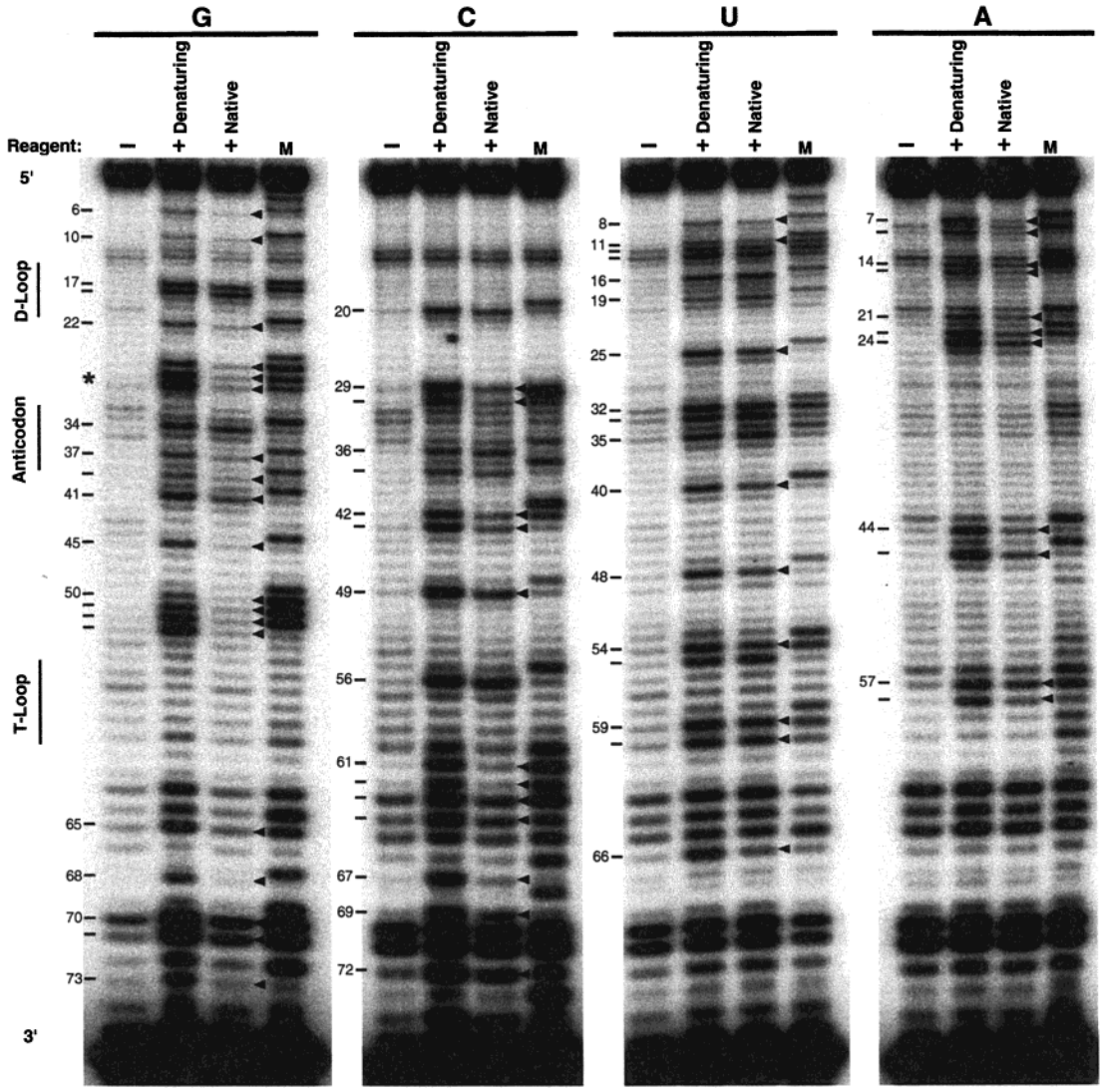

Figure 4. Acylation of 2′-amine substituted $tRNA^{Asp}$ under denaturing and native conditions. Loop regions are identified at left. RNA pools containing 2′-amine substitutions were folded under the conditions specified, treated with **1**, and the 2′-amide product was detected by primer extension. Positions specifically protected under native conditions (10 mM $MgCl_2$, 100 mM NaCl), as compared to reaction under denaturing conditions (50% formamide, 1 mM EDTA), are indicated by arrowheads. Marker lanes (M) were generated by dideoxy sequencing. Bands corresponding to residues G26−28 and G30 (marked with an asterisk) are not fully resolved (see Figure 3 legend), in this gel system.

2′-Amine positions protected from modification under native conditions are superimposed on a secondary structure model of $tRNA^{Asp}$ in Figure 5A and visualized quantitatively in three dimensions in Figure 5B. Inspection of Figure 5 emphasizes that helices and most noncanonical tertiary interactions are protected from acylation at the 2′-amine position. Tertiary interactions are detected independent of whether the interaction involves direct bonding to the 2′-ribose group.

Acylation Detects Folding Transitions in RNA. Native tRNA tertiary folding requires magnesium ion binding at physiological monovalent salt concentrations.[43−45,57] We used selective acylation of 2′-amine positions in $tRNA^{Asp}$ transcripts to map local conformational changes as a function of magnesium ion concentration. Given that acylation is sensitive to local nucleotide flexibilities and that the reaction is not effected by magnesium ion concentration (Table 1), changes in 2′-amine reactivity directly reflect magnesium ion-induced RNA folding. Representative data for acylation of 2′-amino-guanosine substituted $tRNA^{Asp}$, as a function of magnesium ion concentration, is shown in Figure 6A. Two distinct folding transitions are detected by selective acylation (identified at right as i and ii). First, a number of positions are relatively unreactive at 100 mM NaCl (in the absence of $MgCl_2$) as compared with denaturing conditions (Figure 6A, transition i). These include nucleotides in the acceptor, anticodon, and T- stem helices and residues in the T- and variable loops. A second transition is detected for D-stem nucleotides and most residues involved in tertiary contacts upon addition of greater than 1 mM $MgCl_2$ (Figure 6A, transition ii). For example residues G50 to G53, which form the T-stem, are strongly protected in the presence of 100 mM NaCl, whereas nucleotide G22 is protected only upon addition of greater than 1 mM $MgCl_2$. In contrast, nucleotides G17, G18, and G34 are reactive under all conditions, indicating that these positions are not involved in stabilizing interactions.

Analogous experiments for transcripts containing 2′-amino-uridyl, adenyl, and cytidyl substitutions identified the same two distinct transitions (data not shown). Results for all nucleotides are summarized schematically in Figure 6B. In the absence of magnesium ion (100 mM NaCl) all helical stems, except the D-stem, are stable (heavy line in Figure 6B). With the addition of greater than 1 mM $MgCl_2$, the D-stem and most residues

(57) Stein, A.; Crothers, D. M. *Biochemistry* **1976**, *15*, 160−168.

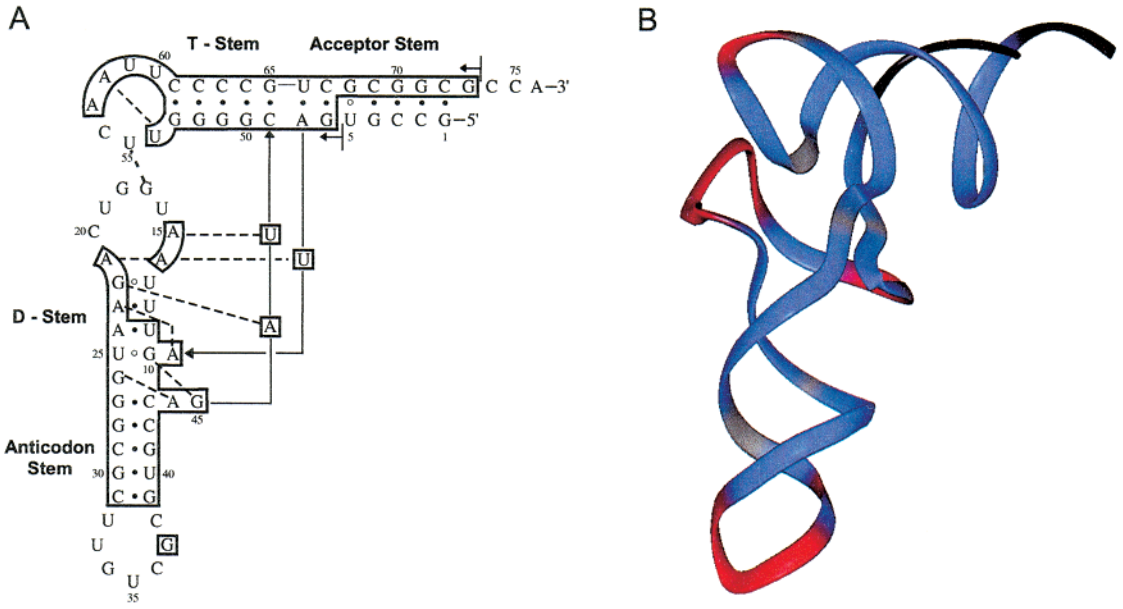

Figure 5. tRNA^{Asp} local nucleotide flexibility determined by selective acylation of 2′-amine substituted nucleotides. (A) Residues protected from acylation under native conditions as compared to denaturing conditions are boxed. Protection is defined as a relative reactivity ($I_{native}/I_{denaturing}$) < 0.65. (B) Visualization of relative acylation reactivities superimposed on the three-dimensional structure of tRNA^{Asp}. Red, gray and blue correspond to nucleotides with relative reactivities ($I_{native}/I_{denaturing}$) of >0.65, 0.65−0.45, and <0.45, respectively. tRNA^{Asp} positions not evaluated in this work are black. Relative reactivities were calculated from band intensities resolved by primer extension after correcting for background.

involved in tertiary interactions become relatively unreactive (light line in Figure 6B). There are also a few residues (G6, A7 and C42 to A46) whose selective acylation reflects contributions from both transitions. For example, residue G45 is clearly protected at 100 mM NaCl, as compared to denaturing conditions, and is further protected upon the addition of $MgCl_2$.

Discussion

Acylation of 2′-amine positions in RNA is sensitive to the extent of local nucleotide flexibility. We find that nucleotides involved in base-pairing or constrained by tertiary interactions are less reactive toward activated esters as compared with nucleotides in loop regions. We exploited this chemistry to obtain a nucleotide resolution picture of differences in the local flexibility of tRNA^{Asp} and to map magnesium ion-induced structural transitions.

Comparison with Crystallographic and Biochemical Studies. To evaluate the utility of our method for monitoring nucleotide flexibilities throughout an entire tRNA molecule, we compared the relative acylation reactivities of 2′-amine groups with crystallographic temperature factors.[46] Temperature factors, a relatively robust measure of local structural flexibility, are related to the root-mean-square displacement of atoms in a crystal determined during refinement.[24,25] We compared the temperature factors for ribose units[46] obtained from refinement of tRNA^{Asp} with relative reactivities calculated by dividing individual band intensities for reaction under native conditions with reaction under denaturing conditions ($I_{native}/I_{denaturing}$). Since temperature factors are restrained to minimize variation between neighboring residues, we compared temperature factors to averaged relative reactivities (using a three-nucleotide window).

Relative reactivities for 2′-amine positions under native conditions show qualitatively the same profile as residue averaged crystallographic temperature factors (Figure 7). Loop regions are less defined in the tRNA^{Asp} crystal, whereas base-paired regions are more precisely resolved, as reflected by their temperature factors. Acylation of 2′-amine positions exhibits an analogous pattern in which loop regions are more reactive

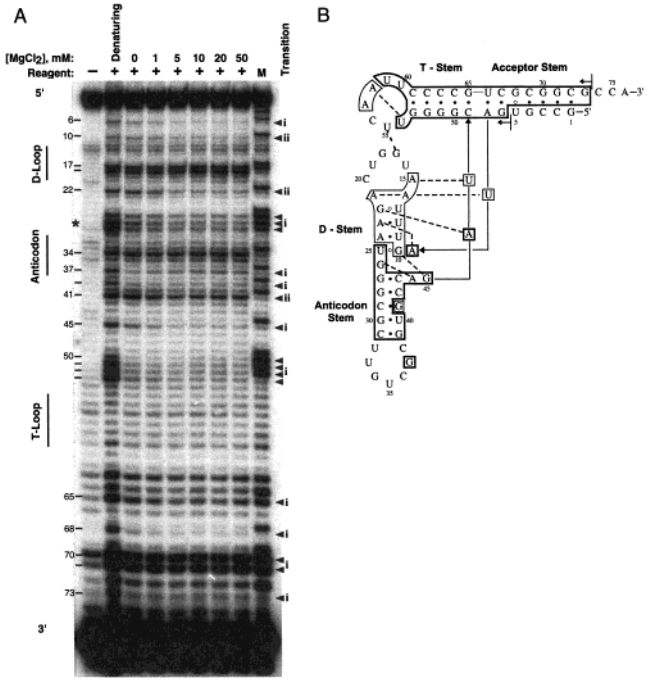

Figure 6. Magnesium ion-induced folding transitions in tRNA^{Asp}. (A) Representative data for acylation of 2′-amino-guanosine substituted tRNA^{Asp}. Loop regions and guanosine residue positions are identified at left. Symbols i and ii, at right, refer to RNA structural transitions between (i) denaturing and 100 mM NaCl conditions (absence of $MgCl_2$) and (ii) 1 mM and 5 mM $MgCl_2$, respectively. (B) RNA folding transitions superimposed on a secondary structure model of tRNA^{Asp}. Regions protected at 100 mM NaCl and at greater than 1 mM $MgCl_2$ are shown with heavy and thin lines, respectively.

than base-paired helices. Moreover, the T-loop is measurably less flexible than the anticodon and D-loops, as judged by both 2′-amine acylation and temperature factors. The 2′-amine acylation data exhibit greater local variation and a few positions at which reaction is faster than would be predicted from temperature factors. These differences may be due to the absence

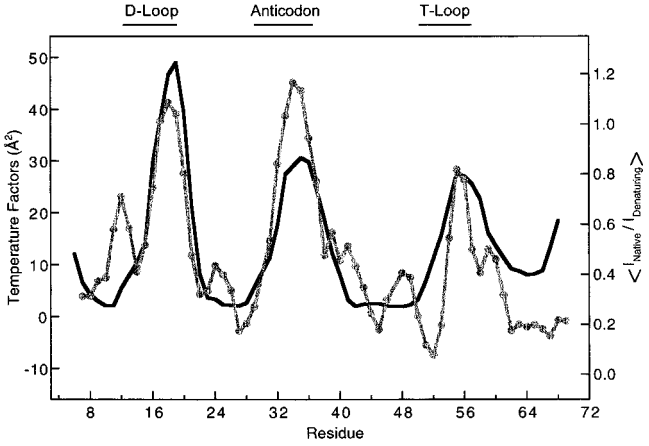

Figure 7. Comparison of relative reactivities, $I_{native}/I_{denaturing}$, for acylation of 2′-amine groups (gray line, closed circles) with crystallographically determined temperature factors[46] (dark line, no symbols). Temperature factors were averaged over the ribose unit and were constrained during refinement to minimize differences between neighboring residues. To facilitate comparison, relative reactivities are averaged over a three-residue window.

of stabilizing modified nucleotides present in the crystallized RNA or to crystal packing effects.[23,58]

Acylation of 2′-amine substituted tRNA^{Asp} yields a solution structure that agrees closely with prior work on tRNA^{Asp} transcripts lacking post-transcriptional modifications in which the A, G, and C bases were modified with diethylpyrocarbonate (DEPC) and dimethylsulfate (DMS).[23] Both approaches detect stable base pairs in the acceptor and T-stems and detect most tertiary interactions observed in the crystal structure.[46,47] However, we find that the anticodon stem is stable, as observed in crystallographic studies[46,47] and imino proton resonance experiments[27] on native tRNA^{Asp}. We also find that uridine residues in the D-stem, which are not monitored using DMS or DEPC, exhibit a relatively high level of reactivity as compared to other base-paired nucleotides. An unexplained difference is the reproducible protection of G37 in the anticodon loop, which is reactive toward DMS and lead ion-induced strand cleavage.[23,43]

Interdependent Formation of the D-Stem Helix and Tertiary Interactions in tRNA^{Asp}. Acylation of 2′-amine modified tRNA^{Asp}, as a function of magnesium ion concentration, identifies two clear folding transitions. First, in the presence of 100 mM NaCl (absence of $MgCl_2$) all canonical helices form stably except the D-stem. Second, upon the addition of greater than 1 mM $MgCl_2$ (at 100 mM NaCl) residues in the D-stem and those involved in most tertiary interactions become protected from acylation (Figure 6).

Using NMR, Choi and Redfield[45] have detected similar transitions where (i) in the absence of magnesium (100 mM NaCl, 100 mM sodium phosphate pH 7.0), the T- and anticodon stems show no change in proton amide exchange rates up to 45 °C, but there is a simultaneous melting of D-stem and tertiary interactions (base pairs U8:A14, T54:A58, and A15:U48) at 39 °C, (ii) addition of 1 mM $MgCl_2$ elevates the melting temperature of the D-stem and tertiary contacts to 43 °C, and (iii) at 6 mM $MgCl_2$ they detect a single melting temperature of 45 °C for the entire molecule except for base pair G30:U40.

Thus, as judged by both selective 2′-amine acylation and NMR proton amide exchange, formation of the native tertiary structure is energetically interdependent with stable helix formation in the D-stem. Coupled formation of base-paired helices and tertiary interactions has also been observed for folding of tRNA^{fMet},[57] of a pseudoknotted mRNA fragment[59] and of the P5abc subdomain of the Tetrahymena ribozyme.[60]

2′-Amine Acylation Is Gated by RNA Structure. The distinct pattern of acylation of 2′-amine substituted RNA contrasts sharply with Fe(II)-EDTA mediated hydroxyl radical cleavage. Both reagents react at the RNA backbone; however, unlike 2′-amine acylation, hydroxyl radical cleavage of the phosphoribose backbone is correlated with static solvent accessibility.[20,61,62] For example, in the case of tRNA^{Phe} the solvent-accessible backbone of the anticodon stem is cleaved by hydroxyl radicals,[20] but the analogous structure in tRNA^{Asp} is unreactive with respect to 2′-amine acylation (Figure 4). Thus, an alternative mechanism is required to explain the sensitivity of the 2′-amine acylation reaction to local nucleotide flexibility in RNA.

2′-Amine acylation within an RNA molecule can be described by a model in which reaction is gated by the underlying RNA structure (Scheme 2). Individual regions within the RNA exist in an equilibrium between an unreactive, closed state and a reactive, open state. RNA residues in the open state are acylated irreversibly to form the 2′-amide product. Under our conditions, reaction is very slow ($k_{obs} \approx 0.13$ min^{-1} at 50 mM ester, see Table 1) compared to microsecond and millisecond time scales expected for local RNA nucleotide breathing, flipping, and opening reactions.[4,33] Thus, the observed rate of reaction is given by $k_{obs} = K_{co}k_{acyl}$, where K_{co} describes the closed to open equilibrium and is less than unity for constrained residues. By this mechanism, acylation of 2′-amine substituted RNA would be analogous to proton amide exchange experiments.[44,45,63]

Scheme 2

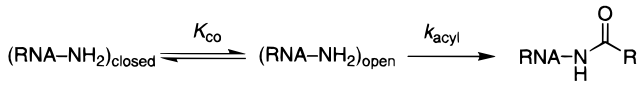

In sum, acylation of 2′-amine substituted RNA monitors local nucleotide flexibility within RNA molecules. Since the intrinsic rate of acylation is independent of $MgCl_2$ concentration, this method represents a useful approach for monitoring magnesium ion-dependent RNA folding. Here the approach illustrates that D-stem helix formation and global tertiary folding are coupled for tRNA^{Asp} transcripts. The advantage of this chemical approach is the potential to monitor, at nucleotide resolution, the folding of an entire RNA molecule of any size through a simple, one step modification. Although the use of a 2′-amine analogue may introduce a small structural perturbation, the excellent correlation between known tertiary interactions in tRNA^{Asp} with protection from acylation (Figure 5A) suggests this effect is small. This approach will be especially useful for evaluating the effects of protein, ion, and other ligand binding on RNA structure.

Experimental Section

RNA Oligonucleotide Synthesis and Purification. Oligoribonucleotides, including a singly substituted 2′-amino cytidyl oligonucleotide, were synthesized and partially purfied at the Nucleic Acid Facility at

(58) Moras, D.; Dock, A.-C.; Dumas, P.; Westhof, E.; Romby, P.; Ebel, J.-P.; Geige, R. *Proc. Natl. Acad. Sci. U.S.A.* **1986**, *83*, 932−936.
(59) Gluick, T. C.; Draper, D. E. *J. Mol. Biol.* **1994**, *241*, 246−62.
(60) Wu, M.; Tinoco, I. *Proc. Natl. Acad. Sci. U.S.A.* **1998**, *95*, 11555−11560.
(61) Murphy, F. L.; Cech, T. R. *J. Mol. Biol.* **1994**, *236*, 49−63.
(62) Cate, J. H.; Gooding, A. R.; Podell, E.; Zhou, K.; Golden, B. L.; Kundrot, C. E.; Cech, T. R.; Doudna, J. A. *Science* **1996**, *273*, 1678−1685.
(63) Bai, Y.; Englander, J. J.; Mayne, L.; Milne, J. S.; Englander, S. W. *Methods Enzymol.* **1995**, *259*, 344−356.

North Carolina State University on a PE Biosystems ABI 394 RNA/DNA synthesizer using standard phosphoramidite methods for synthesis and deprotection.[64,65] The 2′-amino-2′-deoxy-cytidyl phosphoramidite was obtained from Glen Research. All oligomers were purified by denaturing electrophoresis [20% polyacrylamide, 29:1 acrylamide: bisacrylamide, 7 M urea, TBE (90 mM Tris-borate, 2 mM EDTA), 2 h, 30 W]; excised from the gel; electroeluted (using an Elutrap, Schleicher and Schuell, in $^1/_2\times$ TBE, 150 V, 4 h); ethanol precipitated; resuspended in TE (10 mM Tris, pH 7.5, 1 mM EDTA); and stored at −20 °C.

Acylation of Single Stranded, Duplex, and Mismatched Substrates. The 2′-amino-2′-deoxy-cytidyl-substituted oligoribonucleotides (5′-UGUAUUCCU-C-GCCUGUCCAG-3′; site of 2′-amine substitution is underlined) and the corresponding all-ribose oligomer were 5′-^{32}P-end-labeled using T4 polynucleotide kinase and [γ-^{32}P]ATP;[66] purfied on a 20% denaturing gel; recovered overnight at 4 °C by elution in 500 mM potassium acetate (pH 6.0) and 1 mM EDTA; precipitated with ethanol, resuspended in TE, and stored at −20 °C.

All reactions followed the same general procedure in which the oligonucleotide substrate was denatured by heating at 95 °C for 3 min in TE, cooled to room temperature over 20 min for annealing, and subsequently equilibrated with a buffer solution by heating at 37 °C for 5 min. Reactions were initiated by adding 1 μL of sulfosuccinimidyl-6-(biotinamido)hexanoate (500 mM in dimethyl sulfoxide (DMSO), 10 μL total reaction volume) and were then incubated at 37 °C for a specified time. Sulfosuccinimidyl-6-(biotinamido)hexanoate and succinimidyl-6-(biotinamido)hexanoate were obtained from Pierce. Final reaction conditions were 100 mM HEPES/sodium acetate/MES buffer (pH 8.0), 100 mM NaCl, $MgCl_2$ as specified, and 10% DMSO. Reactions were quenched by adding 15 μL of a 333 mM dithiothreitol (DTT), 53% formamide solution and placed on ice. Control reactions contained 1 μL of DMSO without reagent and were incubated for either 60 or 90 min. Products were resolved using a strongly denaturing polyacrylamide gel (15% polyacrylamide, 29:1 acrylamide:bisacrylamide, 4 M urea, TBE, ∼30% v/v formamide, 65 W, 3.5 h; gel dimensions 0.75 mm × 31 cm × 38.5 cm). Band intensities were quantified using a Molecular Dynamics Storm 840 Phosphorimager.

The selectivity of acylation of 2′-amine modified sites within an RNA molecule was determined by comparing the reactivity of the oligonucleotide that contained either all ribose nucleotides or a single 2′-amino cytidyl residue. Reactions contained labeled oligonucleotide (2000 cpm) and 10 mM $MgCl_2$.

Acylation rates for single-stranded, duplex, and mismatched substrates were analyzed as a function of both $MgCl_2$ concentration and reagent charge (anionic versus neutral). All reactions contained the single 2′-amine cytidyl substituted oligonucleotide. Reactions of duplex and mismatched helices contained 0.72 μM of a complementary (5′-CUGGACAGGCGAGGAAUACA-3′) or mismatched (5′-CUGGACAGGC-A-AGGAAUACA-3′, mismatch is underlined) strand. For 0 min time points the DTT-containing quench solution was added prior to the ester. Final $MgCl_2$ concentrations of 0, 1, 5, 10, 20, and 50 mM were tested. For reactions in which reagent charge was tested, a 20 mM final ester concentration (10% DMSO) was used for both the neutral (succinimidyl-6-(biotinamido)hexanoate) and anionic (sulfosuccinimidyl-6-(biotinamido) hexanoate) ester, due to decreased solubility of the neutral ester in aqueous solution. Reactions for the anionic and neutral ester were performed in the absence of $MgCl_2$ over 90 min.

Control experiments, in which the reagent was incubated in reaction buffer omitting the 2′-amine containing oligonucleotide, demonstrated that the succinimidyl ester undergoes inactivation by hydrolysis in parallel with 2′-amine acylation. For the slower reactions of the mismatched and duplex substrates, reaction endpoints were always significantly less than 100%, even for very long reaction times, due to reagent inactivation by hydrolysis. The mechanism describing these parallel pathways is shown in Scheme 3, where A represents the activated ester, R is the RNA substrate and X represents the hydrolysis products of the succinimidyl ester (*N*-hydroxy(sulfo)succinimide and *N*-(+)-biotinyl-6-amino caproic acid). For this mechanism, formation of the acylated product is given by

$$fraction\ R_{acyl} = 1 - \exp\left\{\frac{k_{acyl}}{k_{hydrolysis}}(e^{-k_{hydrolysis}t} - 1)\right\}$$

where k_{acyl} and $k_{hydrolysis}$ are the pseudo-first-order rate constants for acylation and reagent hydrolysis, respectively. Data were initially subjected to a two-parameter fit, and the global rate of reagent hydrolysis was determined to be 0.025 min^{-1}. This value for $k_{hydrolysis}$ was then fixed and used in a single parameter fit to determine k_{acyl} for single-stranded, duplex, and mismatched substrates.

Scheme 3

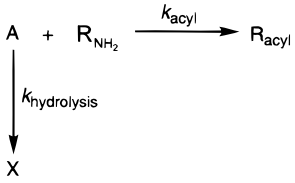

tRNA^{Asp} Synthesis. RNAs were synthesized enzymatically using T7 RNA polymerase[49] and a DNA template generated by PCR. Transcription reactions (300 μL, 37 °C, 2 h) contained 40 mM Tris-HCl (pH 8.0), 10 mM $MgCl_2$, 10 mM DTT, 2 mM spermidine, 0.01% Triton, 4% poly(ethylene glycol) 8000,[54] DNA template, 0.1 mg/mL T7 RNA polymerase, and 2 mM of each nucleotide triphosphate. To generate RNAs containing single 2′-amine substitutions, reactions contained 1.2 mM of the desired 2′-amino-2′-deoxy nucleotide triphosphate (Amersham) and 0.8 mM of the ribonucleotide triphosphate. RNAs were purified on 8% denaturing, polyacrylamide gels and electroeluted as described above.

tRNA^{Asp} Modification: Native. RNA (1.0 pmol) was denatured by heating at 95 °C for 3 min in TE and then refolded by incubation in 100 mM HEPES/sodium acetate/MES buffer (pH 8.0), 100 mM NaCl and 10 mM $MgCl_2$ at 37 °C for 20 min. Reactions (10 μL) were initiated by addition of 1 μL of sulfosuccinimidyl-6-(biotinamido)hexanoate (500 mM in DMSO) and incubated at 37 °C for 15 min. Reactions were quenched by addition of 55 mM DTT in 90 μL of a 220 mM NaCl, 1.67 mM EDTA, and 220 μg/mL glycogen solution; precipitated with ethanol; washed with 80% EtOH; and stored in TE buffer at −20 °C. Control reactions contained 1 μL of DMSO without reagent. The biotin moiety linked to the succinimidyl ester is not required for the present study, per se; however, use of the bulky side chain yields a clearer pattern of stops when analyzed by primer extension. For reactions performed as a function of [$MgCl_2$] RNAs were renatured and modified in 100 mM HEPES/sodium acetate/MES buffer (pH 8.0), 100 mM NaCl supplemented with the required concentration of $MgCl_2$ (0, 1, 5, 10, 20 or 50 mM).

Denaturing Conditions. RNA (1.0 pmol) in 100 mM HEPES/sodium acetate/MES buffer (pH 8.0), 1 mM EDTA, and 50% (v/v) formamide was heated at 95 °C for 1 min, treated with 1 μL of sulfosuccinimidyl-6-(biotinamido)hexanoate (500 mM in DMSO, 10 μL total reaction volume), and incubated at 50 °C for 15 min. Reactions were quenched by addition of 55 mM DTT in 90 μL of a 220 μM NaCl and 220 μg/mL glycogen solution followed by ethanol precipitation of the RNA and final storage in TE buffer at −20 °C.

Primer Extension. The oligodeoxynucleotide primer (5′-CGCTC-TAACTGTTTTCACTT-3′) was purified by denaturing electrophoresis on a 20% gel; excised and eluted from the gel overnight at 4 °C in 500 mM potassium acetate (pH 6.0) and 1 mM EDTA; and 5′-^{32}P-end-labeled using T4 polynucleotide kinase and [γ-^{32}P]ATP.[66]

RNA (0.1 pmol) and 0.4 pmol primer in 50 mM Tris-HCl (pH 8.3), 60 mM NaCl, and 10 mM DTT were annealed by heating at 95 °C for 3 min followed by slow cooling to room temperature over 20 min. Extension reactions contained 2.5 μL of annealed RNA-primer solution, 1.25 μL of water, and 2.5 μL of 50 mM Tris-HCl (pH 8.3), 60 mM NaCl, 6.25 mM DTT, 17.5 mM $MgCl_2$, 1 mM each dNTP, and 0.06

(64) Wincott, F.; DiRenzo, A.; Shaffer, C.; Grimm, S.; Tracz, D.; Workman, C.; Sweedler, D.; Usman, N. *Nucleic Acids Res.* **1995**, *23*, 2677−2684.

(65) Scaringe, S. A.; Francklyn, C.; Usman, N. *Nucleic Acids Res.* **1990**, *18*, 5433−5441.

(66) Krol, A.; Carbon, P. *Methods Enzymol.* **1989**, *180*, 212−227.

units/μL AMV reverse transcriptase (Boehringer Mannheim).[56] Reactions were incubated at 45 °C for 10 min and quenched with 2 vols of 80% formamide. For dideoxy sequencing, reactions contained 500 μM ddNTP. Samples were heated at 95 °C for 3 min and resolved on an 8% denaturing gel (gel dimensions 0.75 mm × 31 cm × 38.5 cm). Bands within the G26 to G30 region were not fully separated using a denaturing, 7 M urea gel, but can be resolved using a strongly denaturing polyacrylamide gel [8%, 29:1 acrylamide:bisacrylamide, 6 M urea, TBE, formamide to volume (~50%)] (see Figure 3, inset). For our analysis, we assumed that residue G30 had a relative reactivity comparable to that of G26-G28.

Conditions for the Incorporation of a Single 2′-Amino Modified Nucleotide per RNA Transcript. A 10-mer oligonucleotide (GCCGC-U_X-AAA) containing a unique uridyl residue was used to determine the efficiency of incorporation of 2′-amine substituted nucleotides using T7 RNA polymerase. RNAs were transcribed with varying ratios of UTP to 2′-amino-2′-deoxy UTP. Transcription reactions (10 μL; 37 °C, 1 h) contained 40 mM Tris-HCl (pH 8.0), 5 mM DTT, 1 mM spermidine, 15 mM $MgCl_2$, 0.01% Triton, DNA template, 1 mM CTP, 1 mM GTP, 250 μM ATP, ~10 μCi [α-^{32}P]ATP, 0.1 mg/mL T7 RNA polymerase and a total concentration of 1 mM UTP and 2′-amino-2′-deoxy-UTP. RNAs were purified from 20% gels and passively eluted; RNA transcripts containing a single 2′-amino modified UTP were subsequently resolved from ribouridine transcripts using an acidic, polyacrylamide gel system (20% polyacrylamide, 29:1 acrylamide: bisacrylamide, 7 M urea, 50 mM potassium acetate (pH 5.6), 7.5 h at 20 W). Transcripts containing 2′-amino-2′-deoxy uridine were effectively separated from ribouridine transcripts, due to protonation of the 2′-amine group. A 2′-amino-2′-hydroxyl UTP ratio of 1.5:1 yields an incorporation efficiency in the final transcript of $\ll$0.05. Extrapolated to the $tRNA^{Asp}$ transcript containing 18 uridine residues, this level of substitution will yield at most a single 2′-amine moiety per transcript.

Acknowledgment. We thank Eric Westhof for providing accessibilities for 2′-ribose positions, Holden Thorp and members of the Weeks laboratory for careful readings of the manuscript, Debbie John for invaluable experimental input and purification of oligoribonucleotides, Nancy Thompson for discussion of the kinetics of reagent inactivation, and Traci Hall for assistance with Figure 5B. This research was supported by the NIH (GM56222) and by a Research Innovation Award from Research Corporation. K.M.W. is a Searle Scholar of the Chicago Community Trust.

JA9914137